Lateral Diffusion of Redox Components in the Mitochondrial Inner Membrane Is Unaffected by Inner Membrane Folding and Matrix Density*

Brad Chazotte‡ and Charles R. Hackenbrock

From the Department of Cell Biology and Anatomy, Laboratories for Cell Biology, School of Medicine, University of North Carolina, Chapel Hill, North Carolina 27599-7090

We report the first lateral diffusion measurements of redox components in normal-sized, matrix-containing, intact mitoplasts (inner membrane-matrix particles). The diffusion measurements were obtained by submicron beam fluorescence recovery after photobleaching measurements of individual, intact, rat liver mitoplasts bathed in different osmolarity media to control the matrix density and the extent of inner membrane folding. The data reveal that neither the extent of mitochondrial matrix density nor the complexity of the inner membrane folding have a significant effect on the mobility of inner membrane redox components. Diffusion coefficients for Complex I (NADH:ubiquinone oxidoreductase), Complex III (ubiquinol: cytochrome *c* oxidoreductase), Complex IV (cytochrome oxidase), ubiquinone, and phospholipid were found to be effectively invariant with the matrix density and/or membrane folding and essentially the same as values we reported previously for spherical, fused, ultralarge, matrix-free, inner membranes. Diffusion of proton-transporting Complex V (ATP synthase) appeared to be 2–3-fold slower at the greatest matrix density and degree of membrane folding. Consistent with a diffusion-coupled mechanism of electron transport, comparison of electron transport frequencies (productive collisions) with the theoretical, diffusion-controlled, collision frequencies (maximum collisions possible) revealed that there were consistently more calculated than productive collisions for all redox partners. Theoretical analyses of parameters for submicron fluorescence recovery after photobleaching measurements in intact mitoplasts support the finding of highly mobile redox components diffusing at the same rates as determined in conventional fluorescence recovery after photobleaching measurements in fused, ultralarge inner membranes. These findings support the Random Collision Model of Mitochondrial Electron Transport at the level of the intact mitoplast and suggest a similar conclusion for the intact mitochondrion.

A primary focus of this laboratory continues to be the study of the relationship between the mobility of mitochondrial inner membrane redox components and electron transport.[1] We have previously adopted the technique of FRAP[2] to quantitate the rates of lateral diffusion of specific inner membrane components. This technique usually requires membranes having a diameter >5 μm, whereas the intact rat liver mitochondrion is approximately 1 μm in diameter and the typical isolated, swollen inner membrane averages approximately 1.5 μm. Therefore, we previously developed fusion procedures to produce ultralarge spherical matrix-free inner membranes (10–200 μm) for our FRAP diffusion studies (1, 2). Based upon our determination of the rates of diffusion of the redox components in these ultralarge inner membranes and comparison of the diffusion-based collision frequencies of redox components to electron transport rates, we hypothesized a Random Collision Model for Mitochondrial Electron Transport (3–8). The model (for details see Ref. 4) states that: 1) all redox components are independent diffusants; 2) electron transport is a diffusion-coupled kinetic process, *i.e.* all electron transfers are preceded by one or more diffusion-based collisions; 3) cytochrome *c* diffuses primarily in three dimensions at physiologic ionic strength; 4) electron transport is a multicollisional, obstructed, long range, diffusion process; and 5) the rates of diffusion of redox components have a direct influence on the overall kinetic process of electron transport and can be rate-limiting.

Although the majority of studies to date to assess the diffusion of redox components have been carried out on fused ultralarge mitochondrial inner membranes, a limited number of studies have utilized other enlarged, structurally altered, mitochondrial membrane systems, such as hypotonically swollen, cuprizone-induced megamitochondria from mouse liver (3, 9, 10) and "partly damaged," hypotonically swollen large mitochondria from the flight muscle of *Lethocerus indicus* (11). Because of the technical difficulties related to their small size, no FRAP studies to date have been carried out on intact mitochondria or unswollen, intact, matrix-containing inner membranes, *i.e.* mitoplasts. The small, native mitochondrion and mitoplast are of course preferred for such studies

---

[1] Electron transfer refers to the actual transmission of reducing equivalents between redox components. Electron transport is inclusive of the overall process of electron transfer and lateral diffusion of redox components.

[2] The abbreviations used are: FRAP, fluorescence recovery after photobleaching; BSA, bovine serum albumin; Hepes, 4-(2-hydroxyethyl)-1-piperazineethanesulfonic acid; asolectin, soybean phospholipids; DiI, 3,3'-dioctyldecylindocarbocyanine; TRITC, tetramethylrhodamine B isothiocyanate; Complex I or I, NADH:ubiquinone oxidoreductase; Complex II or II, succinate:ubiquinone oxidoreductase; Complex III or III, ubiquinol:cytochrome *c* oxidoreductase; Complex IV or IV, cytochrome oxidase; Complex V or V, ATP synthase; Q, ubiquinone; *c*, cytochrome *c*; *D*, lateral diffusion coefficient.

since they are both structurally and functionally intact. The outer surface of the mitoplast's inner membrane is accessible to immunofluorescence labeling of its integral protein complexes since the outer membrane is absent. Both the mitoplast and the mitochondrion have a matrix that in different metabolic states can vary from an ~27% protein "solution" in the orthodox configuration to 56% in the condensed configuration and can potentially interact with the redox complexes that project out from the inner membrane surface. Concomitantly, the extent of inner membrane folding will vary significantly. Together or separately, matrix density and inner membrane folding each have the potential to significantly affect the rate of diffusion of inner membrane components. Therefore, it is a progressive, yet essential step to attempt to examine these physical factors.

In this report, we extend our FRAP techniques to individual, intact matrix-containing mitoplasts from rat liver mitochondria measuring ~1–3 μm at different osmolarities in order to consider the potential effects of the mitochondrial matrix and/or inner membrane folding on diffusion rates that could not be directly addressed previously. We determined that all diffusants studied in the inner membrane of intact, matrix-containing mitoplasts are highly mobile. With the possible exception of the proton-transporting ATP-synthase, which is not involved in electron transport, we found no significant differences in the rates of diffusion of specific mitochondrial inner membrane redox (electron transporting) components or phospholipids between fused, ultralarge, matrix-free inner membranes and mitoplasts over a range of osmotic conditions which dramatically alters inner membrane folding and matrix density. We conclude that the matrix density and inner membrane folding do not have a significant effect on the diffusion of mitochondrial inner membrane redox components and electron transport.

EXPERIMENTAL PROCEDURES

Membrane Preparations—Mitochondria were isolated from the livers of male Sprague-Dawley rats based upon previously published procedures using H_{300} isolation medium (300 mosm medium containing 220 mM mannitol, 70 mM sucrose, 2 mM Hepes, and 0.5 mg/ml bovine serum albumin at pH 7.4) (12). The outer membranes were selectively removed using a controlled digitonin incubation (13) subsequently leaving a mitoplast fraction. A portion of the mitoplast fraction was converted to a simple spherical shape, and the matrix was diluted approximately 7-fold by washing in a hypotonic 40 mosm H_{40} medium, a 7.5-fold dilution of H_{300} BSA-free medium (14). For electron microscopy studies, samples were suspended in the appropriate isolation medium. Microsamples of 2–5 μl at 4 °C were chemically fixed by centrifuging through 2% glutaraldehyde, pH 7.4, at 9800 × g to form micropellets. Glutaraldehyde-fixed samples were then postfixed for 1 h in phosphate-buffered 2% osmium tetroxide, pH 7.4. Epon-embedded micropellet sections were stained for 5 min in saturated uranyl acetate in 50% ethanol followed by 4 min in lead hydroxide. Thin sections were photographed with a JEOL 100CX electron microscope operated at 60 kV.

Fluorescent Probes and Membrane Labeling—FRAP measurements of Ds for inner membrane components were carried out utilizing fluorescent probes. Phospholipid and ubiquinone diffusion were reported by DiI, as previously reported (5, 6). DiI$_{C:16}$, a fluorescent lipid analogue, was dissolved in EtOH and incorporated into inner membrane suspensions to give a probe/lipid ratio between 1:1,000 and 1:10,000 and a final EtOH concentration of <1%. Immunospecific fluorescent labeling was utilized to monitor redox complex diffusion. Specific rabbit anti-redox complex IgGs were separately prepared utilizing isolated, pure Complexes I, III, IV, and V and were assayed as previously described (15). Complex I was obtained from the late Dr. C. I. Ragan (Merck, Sharpe and Dohme Research Laboratories, Harrow, U. K.), and Complexes III and IV were obtained from the late Dr. T. King. Complex V was isolated as described by Ref. 16. IgGs were conjugated to a lissamine rhodamine sulfonyl chloride or a tetramethylrhodamine isothiocyanate fluorophore as described in

Ref. 3. Mitoplasts attached to glass slides in 300 mosm BSA-free medium were labeled by successive washings with 100 μl of 171 mM NaCl, 20 μl of fluorescent antibody for a 1–2 min incubation, 200–300 μl of NaCl to remove unbound antibody, and finally with 200 μl of H_{300} BSA-free medium. Poly-L-lysine was used to attach and retain the mitoplasts on glass slides during and after the immunofluorescent labeling and washing procedures. For this procedure, acid-washed glass was immersed in 0.1% solutions of the 175-kDa or 1-4-kDa poly-L-lysine and allowed to air dry overnight prior to adding mitoplasts. For experiments using ultralarge, fused inner membranes, a similar labeling procedure detailed previously was used (5).

The structural integrity of the mitoplasts was maintained during isolation and fluorescent labeling using H_{300} medium. For FRAP measurements, the glass-attached mitoplasts were kept in a condensed configuration in H_{300} BSA-free medium or were subsequently converted to a more orthodox configuration in H_{150} (150 mosm) medium or a spherical configuration in H_{40} medium to reduce matrix density and decrease inner membrane folding.

Fluorescence Recovery after Photobleaching—FRAP was carried out by standard methods (17) with some modification, and recovery curves were analyzed by the method of Axelrod *et al.* (18). The instrument described previously (5, 6) was used with the 514.5 nm argon emission line. Submicron FRAP was performed using Leitz 100× brightfield oil immersion lenses with either a 1.30 or 1.32 numerical aperture, each producing beam diameters at the sample plane of <1 μm. Beam diameters were determined by comparison of a stage micrometer image along the direction of both the x and y axes to the fluorescent spot produced on a thin DiI film by a given lens using a digitized video approach with a Dage ISIT video camera (Model 66) and appropriate image processing software. For ultralarge membranes, a Leitz 40× (0.7 Na) dry objective was used as was done previously (5). A Lenzar Intensicon 8 video camera was used to locate the fluorescent inner membranes and focus the laser beam on the membrane surface. The sample temperature was determined by a Sensortek BAT-8 digital thermometer with a thermocouple probe on the microscope stage.

The Ds from recovery curves of 10–20 mitoplasts were averaged. However, to minimize the photobleaching-induced depletion of the fluorophore population due to the small diameter of the mitoplast, fluorescence recovery curves were not signal-averaged for individual mitoplasts during acquisition, and the duration of the bleaching pulse and its intensity were adjusted to give a modest 20–40% average bleach. Due to the very small separation between the upper region and the lower (glass-attached) region of the inner membrane of the mitoplast, it is generally not possible and exceptionally difficult at best to distinguish between them while imaging the laser spot, and it was assumed, and the data indicate, that both membrane regions were bleached and contributed to the observed recovery.

For immobilization of inner membrane components, a 25% stock solution of glutaraldehyde was diluted to 0.2%, 1% and 2% concentrations in H_{300} BSA-free medium. The selected concentration of glutaraldehyde in a 40-μl aliquot was added to glass-slide attached mitoplasts and incubated for 10 min at room temperature. The cross-linking reaction was then stopped with 100 μl of 0.1 M NH$_4$Cl. Immunofluorescence labeling was performed subsequent to cross-linking. For analysis of phospholipid diffusion, DiI was added to bulk membrane suspensions prior to glass attachment and cross-linking.

Electron Transport Activities—Maximum succinate oxidase activities were determined as an average of a number of runs using a Clark-type oxygen electrode (19). The incubation medium was composed of 10 mM potassium phosphate, pH 7.4, 1 μM carbonyl cyanide *m*-chlorophenylhydrazone, and 13 μM cytochrome *c*; 5 mM sodium succinate was used to start the reaction. Membranes were temperature-equilibrated 1–2 min prior to initiating the reaction. Temperatures were read directly in the thermostated oxygen electrode chamber using a Sensortek BAT-12 digital thermometer. The heme content of the cytochromes was determined using the method of Williams (20) and the coefficients of Schneider *et al.* (21). The Lowry method was used to determine the protein concentrations (22).

Theoretical FRAP Calculations—The analyses and equations of Petersen and McConnaughey (23) were used to calculate the effect of two closely opposed membranes on the fluorescence recovery curves. In particular, the case of one membrane (or membrane region) attached to an immobile substratum, analogous to our system, was examined. The beam expansion was calculated based upon a beam radius of 0.48 μm at 514.5 nm for a Leitz 100×, 1.32 NA oil immersion lens, and the collection efficiency for this lens was calculated based on a 200-μm image pinhole and a refractive index of 1.515 for the

immersion oil. An arbitrary bleaching constant and time were selected to produce an ~60% bleach at the image plane. Percent recoveries were selected for the in-focus and out-of-focus membrane regions, and the observed recovery was calculated based upon the following equation

$$F_R^{obs}(z - z_0) = \frac{A^f F_R^f + E(z - z_0)A^o F_R^o}{A^f + E(z - z_0)A^o} \quad (1)$$

where F_R^{obs} is the observed fraction recovery for membranes (or membrane regions) separated by the distance $z - z_0$, F_R^f and F_R^o are the true fractional recoveries, and A^f and A^o are the bleaching efficiencies for the in-focus (f) and out-of-focus (o) membranes, respectively, and $E(z - z_0)$ is the collection efficiency; each calculated as in Petersen and McConnaughey (23).

Materials and Reagents—All reagents were reagent grade. Glutaraldehyde was EM grade and obtained from Electron Microscopy Sciences (Ft. Washington, PA). Cytochrome c (Type VI from horse heart) was purchased from Sigma. Rhodamine isothiocyanate was purchased from Research Organics (Cleveland, OH). DiI and lissamine rhodamine B sulfonyl chloride were obtained from Molecular Probes (Eugene, OR).

RESULTS

Diffusion of Redox Components in Intact Mitoplasts—We determined the Ds of redox Complexes I, III, and IV and Complex V and of both phospholipid and ubiquinone (using DiI) in the inner membranes of intact mitoplasts employing a submicron diameter laser spot (Table I). We found that the average D for each specific inner membrane component was essentially the same, within the limits of experimental error, for intact, matrix-containing mitoplasts compared to ultralarge, fused, matrix-free inner membranes (Table I). The same finding was obtained for small (3–5-μm diameter), fused, matrix-free inner membranes. The size of matrix-free, fused mitoplasts (Table I) or of nonfused, matrix-containing mitoplasts (Table II) did not markedly influence the D of any component. The Ds of the redox components were essentially unchanged regardless of the extent of membrane folding and/or matrix density of intact mitoplasts as the osmotic strength of the medium was lowered from 300 to 40 mosm (Table I). Mitoplasts suspended in solution at 300 mosm are in the condensed state, *i.e.* are irregularly shaped with a high degree of inner membrane folding and have a small volume of dense matrix (Figure 1A), while at 40 mosm the inner membrane unfolds to become spherical and the matrix volume increases (Fig. 1B), giving an approximate 7-fold decrease in matrix density (24). Consistent with our studies using only ultralarge, fused inner membranes, we found Complex I in intact mitoplasts to be the slowest and Complex V to be the fastest integral protein diffusants, and ubiquinone and phospholipid

to be the fastest membrane diffusants. Complex V, which is not involved in electron transport, may diffuse 2–3-fold slower in condensed mitoplasts in 300 mosm medium (mean D: 2.7 $\times$ 10^{-10} cm²/s, Table I) compared to spherical mitoplasts in 40 mosm medium (mean D: 7.3 $\times$ 10^{-10} cm²/s, Table I). Complex I diffused an order of magnitude slower compared to the other complexes in all membranes studied (Table I). These data reveal that the Ds in intact mitoplasts are the same as in fused, ultralarge, matrix-free inner membranes and indicate that neither the matrix nor the extent of inner membrane folding has a significant effect on Ds with the possible exception of the proton-transporting ATP-synthase.

We examined several technical aspects of our approach to measure the Ds of inner membrane components in intact mitoplasts because of the latter's small size of ~1–3-μm diameter. We determined that a low (20–40%) degree of bleaching for two or at most three successive bleaches did not alter the Ds of inner membrane components. We found that the Ds for redox components were not significantly affected by a 0.1% coating on the glass slide of either 1–4-kDa or 175-kDa poly-L-lysine. Poly-L-lysine was required to keep mitoplasts attached to the slides during the labeling and washing procedures, especially for immunofluorescence labeling. We also determined that the incubation of mitoplasts in glutaraldehyde (0.2% or 2%) for 10 min essentially abolished diffusion of all redox components examined (data not shown) which showed that immobilizing interactions of redox components, when present, were clearly discernible. The close agreement of our current and previous results (3) also indicated that submicron FRAP can be successfully applied to accurate and reproducible determinations of Ds in small ~1–3-μm mitoplast membranes attached to glass slides.

Unlike the assessment of Ds, the determination of mobile (and conversely immobile) fractions of inner membrane components in the small mitoplast is problematic for a number of reasons. Although values for significant mobile fractions were obtained in all cases, a precise quantitation for a single, specific membrane is experimentally and theoretically difficult to ascertain. Consequently, an averaging of individual membrane determinations will be subject to similar limitations. Almost all the observed mobile fractions in intact, matrix-containing mitoplasts and fused, matrix-free, small (3–5 μm) mitoplasts for both protein and lipid components tended to be around 50% ± 15% (Table III) as compared to the usual >85% mobile fraction for fused, ultralarge, matrix-free inner membranes. Smaller mitoplasts tended to have somewhat lower mean values, but the differences were within

TABLE I

Comparison of Ds in fused matrix-free inner membranes and matrix-containing mitoplasts

$D \times 10^{10}$ cm²/s at 23 ± 2 °C determined by FRAP as means ± S.D., typically for an average of 10–20 mitoplast membranes.

Membranes	Conditions	Diffusant				
		Phospholipid and ubiquinone (DiI)	Complex I	Complex III	Complex IV	Complex V
	mosm					
Fused, matrix-free, ultralarge >10-μm diameter inner membranes	40	39 ± 9[a]	0.72 ± 0.7	4.4 ± 2.2[b]	3.6 ± 1.7[b]	8.4 ± 6.0[c]
Fused, matrix-free, small 3–5-μm diameter, inner membranes	40			3.4 ± 3.0	3.9 ± 2.2	
Normal, matrix-containing, ~1–3-μm diameter, mitoplasts	40	59 ± 33	0.47 ± 0.2	3.4 ± 2.6	2.5 ± 1.7	7.3 ± 3.0
	150	23 ± 20	0.48 ± 0.2	3.5 ± 2.0	2.6 ± 5.3	6.5 ± 3.5
	300	48 ± 43	0.46 ± 0.3	4.7 ± 3.2	2.8 ± 1.8	2.7 ± 1.2

[a] Ref. 5.
[b] Ref. 3.
[c] Ref. 16.

experimental error (Table II). The mobile fraction was not found to be significantly different whether 1–4-kDa or 175-kDa poly-L-lysine was used to bind the membranes to glass slides, or in the case of phospholipid where labeling with DiI prior to attachment on glass permitted the omission of poly-L-lysine. It was found that the mobile fraction, unlike the *D*, varied to a degree with the degree of bleaching such that the greater the bleach the lesser the mobile fraction. This indicated that the portion of the total inner membrane component-bound fluorophore population bleached was significantly high to reduce the percent recovery. These findings for the mobile fraction of inner membrane components are consistent with: 1) a large proportion of the total membrane surface area of small mitoplasts being photobleached and 2) to an immobilization of inner membrane components due to a significant attachment to the glass substratum; thus, consistent with an *apparent* immobile fraction.

Calculations (Fig. 2A), based on the treatment of Petersen and McConnaughey (23) for our experimental conditions, support our conclusion that the experimentally observed, average, ~50% immobile fraction in the small mitoplasts is only apparent and results from photobleaching two closely separated membranes (*i.e.* the upper and lower regions of the

TABLE II

Effect of mitoplast diameter on Complex III mobility

Diameter	D^a	Mobile fraction
		%
<2	2.1 ± 1.3	43 ± 22
<3	2.5 ± 1.5	49 ± 23
>3	2.9 ± 1.6	59 ± 23

^{a} $D \times 10^{10}$ cm^2/s at 23 ± 2 °C determined by FRAP as mean ± S.D. typically for an average of 20–40 mitoplast membranes. Determined in spherical (40 mosm) mitoplasts.
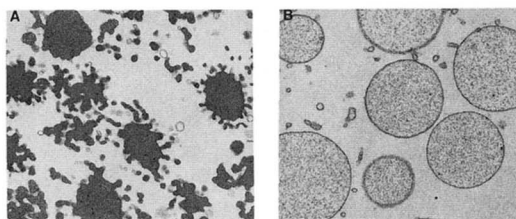

FIG. 1. Thin sections of freshly isolated intact mitoplasts in solution at × 9,810 showing the condensed configuration with a highly folded inner membrane and a dense matrix in 300 mosm isolation medium (*A*). *B*, the spherical configuration with a spherical inner membrane and a dilute matrix in 40 mosm isolation medium.

same mitoplast inner membrane) where one membrane (the lower) has a large proportion of its surface area attached to an immobile substratum. The calculations reveal that over the range of separations between membrane regions of ~0.5 to ~3 μm estimated for intact mitoplasts based on their diameters, an approximately 50% ± 20% observed mobile fraction would be expected (Fig. 2A) resulting from one membrane region (the upper) with a 100% mobile fraction and the other glass-attached membrane region with a 0% mobile fraction. Averaging of a population of membranes where the laser beam spot can be focused on either the mobile or immobile membranes (which are very difficult to distinguish at close separations) would tend to be around 50% ± 20% as we experimentally observed (Table III). At separations greater than 5 μm, typical of conventional spot photobleaching studies, the effect of the attached, immobilized membrane is negligible (Fig. 2B). Although the 100% *versus* 0% mobile fractions case best fit the data, additional calculations were carried out to rule out other possible combinations of mobile fractions for the membranes (data not shown). Thus, the experimental and theoretical analyses of our submicron FRAP studies of intact mitoplasts of ~1–3 μm diameter indicate that the inner membrane redox components are highly mobile and that the 50% immobile fraction is only apparent owing to technical experimental conditions.

Relationship of Electron Transport and Diffusion of Redox Components in Intact Mitoplasts—In the Random Collision Model of Mitochondrial Electron Transport, the significance of diffusion is in the functional collisions between appropriate redox partners. Therefore, we compared the number of diffusion-based collisions calculated by the Hardt equation for two-dimensional diffusion (25) and the number of successful collisions, *i.e.* actual maximum electrons transferred, as done previously (3, 5), and present the results for the intact, condensed mitoplast in 300 mosm medium (Table IV). The diffusion-controlled collision frequencies as well as collision efficiencies were calculated for all redox partners using their FRAP-determined diffusion coefficients and their effective redox concentrations in the mitoplast inner membrane under conditions of maximum (state 3U) respiration. We found that in all cases there were slightly more collisions than electron transfers, closely agreeing with the collision efficiencies in our earlier studies for fused, ultralarge, matrix-free inner membranes. Thus, irrespective of the inner membrane studied, no physical respiratory chain or aggregate, transient or permanent, appears to be required to account for the observed rate or sequence of electron transport. This is based on the crite-

TABLE III

Comparison of mobile fractions in fused matrix-free inner membranes and matrix-containing mitoplasts

Mobile fractions in percent determined by FRAP as mean ± S.D. typically for an average of 10–20 mitoplast membranes. Note that 300 mosm mitoplasts were first attached to glass, the complexes were immunofluorescently labeled, and then the osmolarity was adjusted. The smaller mobile fractions for fused small inner membranes and for mitoplasts are apparent; see text for details.

| Membranes	Conditions	Diffusant				
		Phospholipid and ubiquinone (DiI)	Complex I	Complex III	Complex IV	Complex V
	mosm					
Fused, matrix-free, ultralarge >10 μm diameter inner membranes^a	40	94 ± 5		86 ± 11		
Fused, matrix-free, small 3–5-μm diameter inner membranes	40			53 ± 23	49 ± 28	
Normal, matrix-containing, ~1–3 μm diameter mitoplasts	40	59 ± 33	46 ± 26	69 ± 28	61 ± 23	41 ± 23
	150	46 ± 21	44 ± 30	32 ± 13	42 ± 23	26 ± 11
	300	46 ± 21	58 ± 27	40 ± 30	54 ± 18	41 ± 25

^{a} Chazotte and Hackenbrock (5).
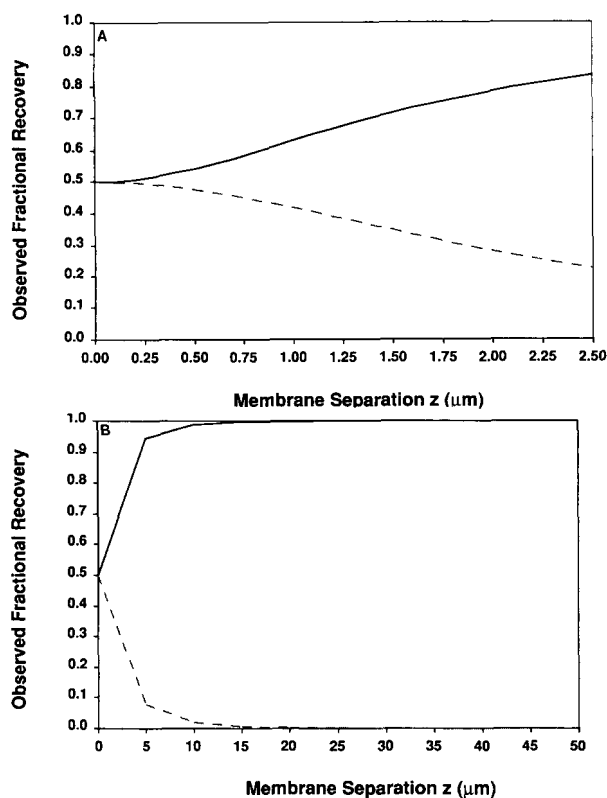
FIG. 2. **Theoretical calculations of observed (apparent) fractional recoveries as a function of different membrane separations for a 100× lens according to the treatment of Petersen and McConnaughey (23).** See "Experimental Procedures" for details. In-focus (upper) membrane with 100% mobile diffusants and out-of-focus (lower) attached membrane with 0% mobile diffusants, ———; in-focus membrane with 0% mobile and out-of-focus with 100% mobile, - - -. *A*, membrane separations 0 to 2.5 μm; *B*, membrane separations 0 to 50 μm.

rion that the resultant collision efficiencies, *i.e.* the number of turnovers/collisions × 100, must be ≤100% for a diffusion-based mechanism to account for the observed rates of overall electron transport.

DISCUSSION

Analysis of the Relationship of Diffusion and Electron Transport in Intact Mitoplasts—The data presented in this communication permit an assessment of the diffusion of redox components and its role in electron transport in the topographically complex, matrix-containing, intact mitoplast which more closely resembles the whole mitochondrion, compared to fused, matrix-free inner membranes used previously. The intact mitoplast, irrespective of configuration, closely approximates the intact mitochondrion functionally and structurally, lacking only the outer membrane and intermembrane space contents. Our findings and analyses indicate that neither the presence of matrix and its density nor the extent of inner membrane folding has a significant effect on the diffusion of mitochondrial inner membrane redox components.

These results on intact, normal size mitoplasts address important, logical questions about the applicability of the Random Collision Model of Electron Transport to the intact mitochondrion that we as well as others have not been able to technically approach. We had previously compared the theoretical number of collisions of appropriate redox partners predicted by their respective diffusion coefficients, effective reduced *versus* oxidized concentrations and collision radius,

with the actual number of successful collisions determined from steady state electron transport rates (turnovers) in spherical, fused, ultralarge, matrix-free inner membranes and found that there was always more predicted collisions than successful collisions (3). Thus, we characterized electron transport as diffusion-coupled, *i.e.* every potentially reactive redox component undergoes one or more diffusion-based collisions with its potentially reactive redox partner to effect one turnover. In addition, we reported that electron transport is a multicollisional, obstructed, long range diffusion process and that the diffusion-based collisions of ubiquinone with its redox partners are rate-limiting for overall succinate-linked electron transport rates (5, 6). Collectively, these findings indicate that any effects on diffusion should in turn affect electron transport rates. Thus, it was essential to determine whether this relationship prevailed in the intact mitoplast which is structurally and functionally more like the intact mitochondrion than is the fused, ultralarge inner membrane. In the present study, in all cases, condensed (300 mosm), orthodox (150 mosm), and spherical (40 mosm) mitoplasts, and for all redox partners, there were consistently more predicted than successful collisions such that collision efficiencies (turnovers/predicted collision × 100) ranged between approximately 2.5 and 44%. Further, for each pair of redox partners, the results were very similar to collision efficiencies obtained in the fused, ultralarge spherical, inner membranes (3, 5). Thus, irrespective of matrix density and/or the extent of membrane folding, all inner membrane components are diffusants, and no respiratory chain or aggregate, transient or permanent, appears to be required to account for the sequence or rate of electron transport.

Our finding that the presence or density of the mitochondrial matrix does *not* have a significant *restrictive* effect on the diffusion of major macromolecular components in the inner membrane suggests that any inner membrane-matrix protein interactions are either limited in extent or duration, weak and/or nonspecific. Previous studies have suggested a structurally organized matrix in association with the inner membrane as determined by electron microscopy of intact chemically fixed mitochondria (14, 26–28) and biochemical studies of isolated components at low, nonphysiological ionic strengths (29–39). Our conclusion regarding the lack of strong inner membrane-matrix interactions are not in conflict with the general concept of sequentially functional matrix enzymes, *e.g.* the tricarboxylic acid cycle, being organized and in close proximity within the matrix proper (29, 30, 37–39). Likewise, our conclusion is not in conflict with the concept of substrate channeling via transient weak interactions (40). Specifically, our diffusion results with rat liver intact mitoplasts indicate that there is no extensive and/or permanent association of organized matrix enzymes with the inner membrane protein complexes. Extensive matrix interactions with inner membrane redox complexes, such as that suggested for Complex I (32), should have a dramatic effect on the lateral diffusion of redox complexes, but no significant effect was detected for any complex. Whatever structure that may exist in the matrix must be either flexible or dynamic enough to undergo extensive ultrastructural transformations that can be energy-linked (26, 27) or osmotically induced (41–43). Based upon hydrodynamic treatments (44), a protein *solution* on the order of 56% in the matrix of the condensed mitochondrion (27) could have a viscous diffusion-retarding effect on large complexes of the inner membrane which project into the matrix. If a large portion of the matrix protein is not in solution but is associated in some matrix structure (27, 29), redox component diffusion might be relatively unaffected,

TABLE IV

Comparison of diffusion, collision, and electron transport frequencies in 300 mosm mitoplasts

Redox component	Lateral diffusion coefficient[a]	Molecules/inner membrane[b]	Reactive area radius[c]	Electrons transferred/turnover	Theoretical diffusion controlled collision frequency[d]		Theoretical diffusion controlled collision frequency	Experimental turnover no.[e]	Collisions/turnover (% collision efficiency)
	cm^2/s		nm		$collisions/s/cm^2$		$collisions/s/cm^2/$ redox partner	$turnovers/s/$ redox partner	
Complex I	4.6×10^{-11}	1,901	4.0	2	I	2.13×10^{13}	15,906	3,360	7.73 (21.1)
					Q		14	3	7.73 (21.1)
Complex II	3.9×10^{-10}	3,801	0.7	2	II	2.98×10^{13}	11,076	1,680	6.59 (15.1)
					Q		20	3	6.59 (15.1)
Ubiquinone	4.8×10^{-9}	119,740	2.5	2	Q	1.80×10^{14}	1,064	27	39.9 (2.50)
					III		2,659	67	39.9 (2.50)
Complex III	4.7×10^{-10}	5,702	4.0	1	III	2.06×10^{13}	1,593[g]	700	2.3 (44.0)
					c		95	42	2.3 (44.0)
Cytochrome c	1.9×10^{-9f}	17,106	4.0	1	c	4.03×10^{13}	1,515[g]	340	4.5 (22.4)
					IV		268	60	4.5 (22.4)
Complex IV	2.8×10^{-10}	13,305							

[a] Based upon FRAP-determined average Ds; Complex II is taken as an average of Complexes III and IV.

[b] Based on 0.19 nmol of heme a/mg of whole mitochondrial protein, a stoichiometry of: 1-I/2-II/3-III/7-IV/63-Q/9-c/14 heme a, 4.3×10^9 mitochondria/mg of protein, monomeric redox components, and on the surface area of an average 1.5-μm diameter spherical inner membrane from morphometric analysis.

[c] Sum of redox partner radii (nm); Complex I, 4.0; Complex II, 0.7; ubiquinone, negligible; Complex III, 2.5; cytochrome c, 1.5; and Complex IV, 2.5.

[d] Two-dimensional diffusion-controlled collision frequency $2\pi C_A C_B \{D_A/\ln[(\pi NC_B)^{-0.5}/a] + D_B/\ln[(\pi NC_A)^{-0.5}/a]\}$ from Hardt (25) corrected for the effective reduced *versus* oxidized concentrations (reduced: 5% Complex I, 5% Complex II, 10% Q, 16% Complex III, 11% c, 20% Complex IV (51).

[e] Based on 48 e^-/s/heme aa_3 during State 3U succinate oxidase respiration at 56 mM ionic strength and adjusted for the effective concentration of the redox partner (51).

[f] Apparent D for lateral diffusion at 56 mM ionic strength from Gupte *et al.* (3).

[g] For the two-dimensional diffusion of cytochrome c concentrated on the membrane surface at 56 mM ionic strength; the more rigorous approach considers the ionic strength-dependent multidimensional diffusion of cytochrome c (7, 8).

unless the complex experienced direct physical contact with the matrix structure. In any case, we observed that only Complex V, which among the complexes has the largest projection into the matrix, may possibly diffuse somewhat slower (2-3-fold) in the condensed mitoplast which contains a matrix density of 56% compared to the spherical mitoplast and fused inner membrane where the matrix density is negligible.

Analysis of Submicron FRAP Measurements—Analyses of our present submicron FRAP studies reveal that mitoplast inner membrane redox components are highly mobile diffusants. The Ds of all components are in close agreement with our previous studies on fused, ultralarge inner membranes and swollen, cuprizone-induced, mouse liver megamitochondria (3, 5, 6) where, in contrast, matrix is lost or greatly reduced in density in both cases. The utility of submicron FRAP for measuring diffusion in the inner membrane of small (~1-3 μm-diameter) intact mitoplasts is supported by the close agreement with our measurements on ultralarge inner membranes and comparison to relevant theoretically based FRAP analyses (23, 45-47). Nonetheless, our interpretation of the data was made cautiously in light of the physical limitations inherent in the assessment of diffusion in such small membranes. We considered the effects on our data of 1) the large size (although <1 μm) of the laser spot relative to the total membrane area, 2) the close apposition of the two membrane regions (one of which was bound to an immobile substratum) which precluded discrimination of the fluorescence signals from the two membrane regions, and 3) the effect of the complex inner membrane surface topography, *i.e.* folding.

The characteristic time (t_c) of the fluorescence recovery in FRAP, from which D is calculated, is essentially independent of the percent recovery (mobile fraction) for an infinite res-

ervoir. However, with a small target the size of a mitoplast, a large proportion of fluorescent diffusants in the membrane are bleached and unavailable to participate in the recovery; thus, the signal/noise ratio could limit the accuracy of the measurements. Therefore, we sought to minimize photobleaching-induced depletion of the fluorophore population in the small mitoplast membrane by not signal-averaging from the same mitoplast and by reducing the extent of bleaching to 20-40%. We determined that up to 2 successive bleaches did not alter the D or the mobile fraction, but greater repetitive bleaching resulted in a progressive loss of signal, consistent with the progressive depletion of the reservoir of unbleached fluorophores. In any case, theoretical analyses by Koppel and Sheetz (45) and by Elson and Qian (47) for a finite fluorophore population calculate a maximum possible overestimate in D of a factor of ~2.

We found D to be largely independent of the separation of the inner membrane's two bleached regions, *i.e.* upper (free) and lower (glass-attached) regions. Although, in the small diameter intact mitoplasts, irrespective of the degree of folding, both regions of the inner membranes are bleached, and fluorescent intensities of both regions are measured, albeit to different degrees. Experimentally, Wu *et al.* (48) found little variance in D for multibilayer membranes. Theoretically, Petersen and McConnaughey (23) showed that for closely opposed membranes the observed D is subject to small variations at most. Furthermore, they showed that if one membrane is immobilized the observed D quite accurately reports the D in the free, unattached membrane. Consistent with these findings our observed Ds were not significantly affected by the degree of closeness of the two opposed inner membrane regions, as determined from comparing the Ds in condensed and spherical mitoplasts. Likewise, the Ds were effectively invariant with the extent of folding. This is consistent with

al. (50) that Ds did not change in the presence or absence of membrane microvilli. Such results are also consistent with the theoretical analysis of Aizenbud and Gershon (46) who determined a maximum calculation error in D of <2-fold lower in the presence of a highly folded membrane surface. Thus, our measurements of Ds in intact mitoplasts represent a valid determination with a maximum theoretical error of approximately 2-fold. However, since membrane folding tends to *underestimate* and the large bleached area relative to the total area tends to *overestimate* Ds *each* by a factor of ~2, the possible error would likely be <2 or mutually canceled out.

All of our observed mobile fractions of all inner membrane components (protein and lipid) were centered around 50% irrespective of whether the mitoplast matrix was present or absent, the membranes were fused or not, or the membranes were folded or spherical. Such results are consistent with the case of two closely opposed membranes with one bound to an immobile substratum and the other ~100% mobile and indicate that the immobile fraction in the present study is only apparent. From our studies using fused ultralarge inner membranes where the glass-attached membrane region is not bleached or monitored and constitutes a lower percent of the total membrane surface area, all inner membrane components show >85% mobile fraction. We compared our results for glass-attached mitoplasts with the 50% mean values for observed mobile fractions calculated according to Petersen and McConnaughey (23) for FRAP of two closely opposed membranes where one membrane is completely or extensively immobilized and the other is ~100% mobile. Consistent with their analysis, our results showed that the accuracy of the observed mobile fraction is far more sensitive to closely opposed membranes and the immobilization of one membrane than is the D. The fact that mobile fractions in our study were partly dependent on the extent of bleaching, *i.e* at high percent bleaching mobile fractions were lower, indicated that a large portion of the total fluorophore population was bleached. It is difficult (*a*) to resolve the two membranes when focusing the laser beam, (*b*) to accurately know the degree of separation at the membrane's two opposing bleached regions, and (*c*) to accurately know the total membrane area (estimated from the diameter in the *x*-*y* plane of the slide). Therefore, it is not possible to definitively and accurately deconvolute the observed apparent mobile fraction into a true mobile fraction for the unattached inner membrane in FRAP measurements of an individual mitoplast. Consequently, an average of a population of mitoplasts, where in-focus membranes could be either the mobile or immobilized membrane region, is likewise affected and will tend to vary about a 50% mean value.

We conclude that diffusion rates of highly mobile redox components in the mitochondrial inner membrane are essentially unaffected by the presence or absence of matrix or the extent of membrane folding. Thus, the concepts postulated in the Random Collision Model of Mitochondrial Electron Transport are valid for the mitoplast, and these can reasonably be extended to include the intact mitochondrion which differs from mitoplasts only in that an outer membrane and components of the intermembrane space are present.

REFERENCES

1. Höchli, M., Höchli, L., and Hackenbrock, C. R. (1985) *Eur. J. Cell Biol.* **38**, 1–8
2. Chazotte, B., Wu, E.-S., Hoechli, M., and Hackenbrock, C. R. (1985) *Biochim. Biophys. Acta* **818**, 87–95
3. Gupte, S. S., Wu, E.-S., Hoechli, L., Hoechli, M., Sowers, A. E., Jacobson, K. A., and Hackenbrock, C. R. (1984) *Proc. Natl. Acad. Sci. U. S. A.* **81**, 2606–2610
4. Hackenbrock, C. R., Chazotte, B., and Gupte, S. S. (1986) *J. Bioenerg. Biomembr.* **18**, 331–368
5. Chazotte, B., and Hackenbrock, C. R. (1989) *J. Biol. Chem.* **264**, 4978–4985
6. Chazotte, B., and Hackenbrock, C. R. (1988) *J. Biol. Chem.* **263**, 14359–14367
7. Gupte, S. S., and Hackenbrock, C. R. (1988) *J. Biol. Chem.* **263**, 5241–5247
8. Gupte, S. S., and Hackenbrock, C. R. (1988) *J. Biol. Chem.* **263**, 5248–5253
9. Hochman, J., Lee, J. G., Schindler, M., and Ferguson-Miller, S. (1985) *Proc. Natl. Acad. Sci. U. S. A.* **79**, 6866–6870
10. Hochman, J., Ferguson-Miller, S., and Schindler, M. (1985) *Biochemistry* **24**, 2509–2516
11. Vanderkooi, J., Marinara, G., and Erecinska, M. (1985) *J. Cell Biol.* **100**, 435–441
12. Schneider, H., Lemasters, J. J., Hoechli, M., and Hackenbrock, C. R. (1980) *Proc. Natl. Acad. Sci. U. S. A.* **77**, 442–446
13. Schnaitman, R., and Greenawalt, J. (1968) *J. Cell Biol.* **38**, 158–175
14. Hackenbrock, C. R. (1972) *J. Cell Biol.* **53**, 450–465
15. Hackenbrock, C. R., Chau, R. M.-W., Hammon, K., and Hoechli, L. (1979) *Methods Enzymol.* **56**, 683–720
16. Gupte, S. S., and Hackenbrock, C. R. (1988) in *Integration of Mitochondrial Function* (Lemasters, J. J., Hackenbrock, C. R., Westerhoff, H., and Thurman, R. G., eds) pp. 95–104, Plenum Press Publishing Co., New York
17. Kapitza, H. G., and Jacobson, K. A. (1985) in *Techniques for the Analysis of Membrane Proteins* (Ragan, C. I., and Cherry, R. J., eds) pp. 345–375, Chapman & Hall Ltd., London
18. Axelrod, D., Koppel, D. L., Schlessinger, J., Elson, E., and Webb, W. W. (1976) *Biophys. J.* **16**, 1055–1069
19. Estabrook, R. W. (1967) *Methods Enzymol.* **10**, 41–47
20. Williams, J. N. (1964) *Arch. Biochem. Biophys.* **107**, 532–543
21. Schneider, H., Lemasters, J. J., Höchli, M., and Hackenbrock, C. R. (1980) *J. Biol. Chem.* **255**, 3748–3756
22. Lowry, O. H., Rosebrough, N. J., Farr, A. L., and Randall, R. J. (1951) *J. Biol. Chem.* **193**, 265–275
23. Petersen, N. O., and McConnaughey, W. B. (1981) *J. Supramol. Struct. Cell. Biochem.* **17**, 213–221
24. Andrews, P. M., and Hackenbrock, C. R. (1975) *Exp. Cell Res.* **90**, 127–136
25. Hardt, S. L. (1979) *Biophys. Chem.* **10**, 239–243
26. Hackenbrock, C. R. (1966) *J. Cell Biol.* **30**, 269–297
27. Hackenbrock, C. R. (1968) *Proc. Natl. Acad. Sci. U. S. A.* **61**, 598–605
28. Pihl, E., and Bahr, G. F. (1970) *Exp. Cell Res.* **63**, 391–403
29. Srere, P. A. (1982) *Trends Biochem. Sci.* **7**, 375–378
30. Srere, P. A. (1987) *Annu. Rev. Biochem.* **56**, 89–124
31. D'Souza, S. F., and Srere, P. A. (1983) *Biochim. Biophys. Acta* **724**, 40–51
32. Sumegi, B., and Srere, P. A. (1984) *J. Biol. Chem.* **259**, 8748–8752
33. Sumegi, B., and Srere, P. A. (1984) *J. Biol. Chem.* **259**, 15040–15045
34. Robinson, J. B., Jr., Inman, L., Sumegi, B., and Srere, P. A. (1987) *J. Biol. Chem.* **262**, 1786–1790
35. Srere, P. A., and Sumegi, B. (1986) *Adv. Exp. Med. Biol.* **194**, 13–25
36. Powers-Lee, S. G., Mastico, R. A., and Bendayan, M. (1987) *J. Biol. Chem.* **262**, 15683–15688
37. Robinson, J. B., and Srere, P. A. (1985) *Biochem. Med.* **33**, 149–157
38. Robinson, J. B., Jr., and Srere, P. A. (1985) *J. Biol. Chem.* **260**, 10800–10805
39. Srere, P. A., Inman, L., Liposits, Z., and Sumegi, B. (1988) in *Integration of Mitochondrial Function* (Lemasters, J. J., Hackenbrock, C. R., Thurmond, R. G., and Westerhoff, H. V., eds) pp. 279–288, Plenum Publishing Co., New York
40. Fukushima, T., Decker, R. V., Anderson, W. M., and Spivey, H. O. (1989) *J. Biol. Chem.* **264**, 16483–16488
41. Stoner, C. D., and Sirak, H. D. (1969) *J. Cell Biol.* **43**, 521–538
42. Garlid, K. D., and Beavis, A. D. (1985) *J. Biol. Chem.* **260**, 13434–13441
43. Halestrap, A. P. (1989) *Biochim. Biophys. Acta* **973**, 355–382
44. Saffman, P. G., and Delbrück, M. (1975) *Proc. Natl. Acad. Sci. U. S. A.* **72**, 3111–3113
45. Koppel, D. E., and Sheetz, M. P. (1983) *Biophys. J.* **43**, 175–181
46. Aizenbud, B. M., and Gershon, N. D. (1982) *Biophys. J.* **38**, 287–293
47. Elson, E. L., and Qian, H. (1989) *Methods Cell Biol.* **30**, 307–332
48. Wu, E.-S., Jacobson, K., and Paphadjopoulos, D. (1977) *Biochemistry* **16**, 3936–3941
49. Wolf, D., Handyside, A. H., and Edidin, M. (1982) *Biophys. J.* **38**, 295–297
50. Dragsten, P., Henkart, P., Blumenthal, R., Weinstein, J., and Schlessinger, J. (1979) *Proc. Natl. Acad. Sci. U. S. A.* **76**, 5163–5167
51. Klingenberg, M., and Kröger, A. (1967) in *Biochemistry of Mitochondria* (Slater, E. C., Kanigu, Z., and Wojtczak, L., eds) pp. 11–20, Academic Press, New York